GOA-1 regulates spermathecal transits

Abstract

G-protein signaling regulates calcium dynamics and contractility in the *C. elegans* spermatheca. G-protein coupled receptors activate heterotrimeric G-proteins, triggering downsteam cascades, including the Gαs-mediated activation of adenylyl cyclase and subsequent Protein Kinase A (PKA) activation. Our previous work identified GSA-1/Gαs and PKA as key modulators of Ca^{2+} oscillations and tissue contractility. In this study, we show that the inhibitory Gαi/o subunit GOA-1 regulates spermathecal transit. We employed TurboID proximity labeling and mass spectrometry to identify 16 candidate interactors of GOA-1. While significant phenotypes were not observed in the spermatheca, these proteins may participate in GOA-1 regulated processes in other tissues.

Description

Heterotrimeric G-proteins are composed of an alpha (α) subunit and a beta-gamma (βγ) subunit, which, when activated by an upstream G-protein coupled receptor (GPCR) or G-protein regulator (GPR), disassociate and independently trigger signaling cascades (Jastrzebska, 2013). In smooth muscle, the activation of Gαs initiates the activation of adenylyl cyclase (AC), which converts adenosine triphosphate (ATP) into 3'-5'-cyclic adenosine monophosphate (cAMP). Protein kinase A (PKA), becomes active when cAMP binds and releases its regulatory subunits. PKA is regulates various metabolic pathways (Lee et al., 2016), cell migration (Howe, 2004), and the relaxation of airway smooth muscle (Billington et al., 2013), among other functions (Sadeghian et al., 2022; Torres-Quesada et al., 2017).

The *C. elegans* spermatheca stores sperm and is the site of fertilization (Figure 1A). In the spermatheca, acto-myosin contractility is stimulated by calcium signaling via the phospholipase PLC-1, which facilitates the release of Ca^{2+} from the endoplasmic reticulum. In previous work, we have identified GSA-1 (Gαs) signaling through PKA as an important regulator of coordinated Ca^{2+} signaling in the spermatheca (Castaneda et al., 2020). Oocyte entry initiates a series of Ca^{2+} oscillations, which eventually lead to contraction and the exit of the fertilized embryo into the uterus. However, several crucial questions remain, such as what initiates this signaling cascade and maintains these Ca^{2+} oscillations and how the combined perception of mechanical and biochemical cues leads to proper response observed at the tissue level.

Here we show that, in addition to GSA-1 (Gαs), GOA-1 (Gi/o), an inhibitory G-protein, also regulates spermathecal contractility. Depletion of GOA-1 by RNAi results in a failure of embryos to exit the spermatheca (Figure 1). To identify regulators and effectors of GOA-1, potentially including the GPCR, we tagged GOA-1 with TurboID (Figure 1B) for proximity labeling. GOA-1::TurboID rescues the locomotion defects of the *goa-1(sa734)* mutant, suggesting the construct is functional. Western blotting confirmed that GOA-1::TurboID successfully biotinylated proteins (Figure 1C). Mass spectrometry analysis was used to identify the labeled proteins. Animals expressing TurboID alone (*goa-1p*::TurboID) and N2s were used as controls. We identified 16 proteins that were biotinylated specifically in triplicate GOA-1::TurboID samples. The volcano plot shows the significance of the proteins' expression relative to controls vs the abundance of the peptides identified (Figure 1D). The identities and homologies of the TurboID targets are shown in Table 1.

We next functionally characterized the GOA-1::TurboID targets for potential roles in transit of oocytes through the spermatheca. Worms expressing GCaMP under the *fln-1* promoter were subjected to RNAi for each of the 16 genes. In this experiment, the percentage of spermathecae

occupied with an oocyte was measured for each gene. If the gene is required for oocyte transit through the spermatheca, the percentage of occupied spermatheca will be higher than the negative control condition. About 20% of the spermathecae were occupied by oocyte in negative control (empty RNAi) while the positive control (*plc-1* RNAi) shows more than 95% spermatheca occupancy (Figure 1E). None of the 16 genes showed a significant spermathecal phenotype.

Although we identified no significant spermathecal phenotype by RNAi, stronger knockdown or analysis of mutant alleles may reveal a role for these genes in the spermatheca. For example, PIEZO1/*pezo-1* does have a known spermathecal phenotype and regulates reproductive tissue contraction (Bai et al., 2020). Moreover, these genes might be useful for studies of GOA-1 interactors in other tissues as interactors were identified using the *goa-1* promoter, from all tissues that expressed that construct. Some of the genes identified may be good candidates for further study, including AQP-1, which is localized on the basolateral membrane in proximity to the G-protein (Huang et al., 2007). NATC-1 expression suggests it may be relevant to contractility regulation in the sheath and distal tip cells (Warnhoff et al., 2014). PBO-4 and TWK-18 are expressed in body wall muscle and are expected to regulate muscle contraction (Beg et al., 2008; Kunkel et al., 2000). The next step is to study if these genes show phenotypes relevant to GOA-1 in other tissues, and if so, to determine whether they interact with GOA-1 in those tissues.

Figure 1: GOA-1 regulates transit of oocytes through the spermatheca. **A)** GOA-1::GFP expression in the hermaphrodite *C. elegans.* Arrows indicate spermathecal expression. (scale bar 100 μm). **B)** TurboID, a BioID derived from *E. coli* biotin ligase, is used for proximity labeling. **C)** Diagram of a GOA-1::TurboID cloning and pull-down of biotinylated proteins by using TurboID proximity labeling. Western blot represents GOA-1::TurboID fusion pull-down with anti-biotin antibody. **D)** A volcano plot indicating significant expression of the proteins in three replicate GOA-1::TurboID samples compared to control. **E)** Population assay of wild type animals grown on control, *plc-1*(RNAi), *gsa-1* (RNAi), *goa-1* (RNAi), and 16 TurboID targets. Spermathecae were scored for the presence or absence of an embryo (occupied or unoccupied) in spermatheca. Stars designate statistical significance (**** $p<0.0001$, *** $p<0.005$, ** $p<0.01$, * $p<0.05$) Figure was made with BioRender.

Table1: Mass spectrometry results of GOA-1 targets and human homology of the TurboID targets from WormBase and NCBI.

***C. elegans* genes**	**Functions**	**Human homology**	**Functions**
alh-3	aldehyde dehydrogenase (NAD+) activity and formyltetrahydrofolate dehydrogenase activity	*aldh1l2*	Mitochondrial 10-formyltetrahydrofolate dehydrogenase
aqp-1	channel activity	*aqp10*	Homotetrameric transmembrane channels
arrd-25	protein transport	*arrdc2*	Unknown
c07d8.6	aldose reductase (NADPH) activity	*akr1c4*	Cytosolic aldo-keto reductase
enol-1	phosphopyruvate hydratase activity	*eno2*	enolase isoenzymes

f38e9.1	phosphoric diester hydrolase activity	*plcxd2*	Phosphatidylinositol catalysis
natc-1	peptide alpha-N-acetyltransferase activity	*naa35*	N-terminal methionine acetylation catalysis
pbo-4	potassium:proton antiporter activity and sodium:proton antiporter activity.	*Slc9a2*	Plasma membrane Na+/H+ antiporter
pes-7	GTPase activator activity; actin filament binding activity; and calmodulin binding activity	*iqgap2*	CDC42 and RAC1 activator, associates with calmodulin
pezo-1	mechanosensitive monoatomic ion channel activity and monoatomic cation channel activity	*piezo2*	Pore-forming mechanosensitive non-specific cation Piezo channel
r102.2	Expressed in neurons.	No homology	N/A
snf-3	amino-acid betaine transmembrane transporter activity	*slc6a1*	gamma-aminobutyric acid (GABA) transport
adh-1	alcohol dehydrogenase (NAD+) activity	*adh4*	NAD-dependent oxidation catalysis
t21b6.3	body wall musculature and muscle cell	*hmcn1*	growth factor beta-mediated rearrangement
twk-18	rectifier potassium channel activity	*kcnk18*	Rectifying K+ channel
vps-26	intracellular protein transport and retrograde transport, endosome to Golgi	*vps26b*	vesicular protein sorting

Methods

C. elegans strains and culture

Nematodes were grown on NGM plates (0.107 M NaCl, 0.25% wt/vol Peptone, 1.7% wt/vol BD BactoAgar, 2.5 mM KPO_4, 0.5% Nystatin, 0.1 mM CaCl 2, 0.1 mM MgSO4, 0.5% wt/vol cholesterol) and fed with *E. coli* OP50 at 23°C. All extra-chromosomal arrays of *goa-1p*::GOA-1::TurboID (20 ng/ul), *goa-1p*::TurboID (10 ng/ul), and an injection marker (50 ng/ul) were injected into N2 animals. Transgenic animals were integrated by UV radiation. Strains used are *goa-1p*::GOA-1::TurboID (UN2301), *goa-1p*::TurboID, (UN2306), *fln-1p*::GCaMP (UN1108), *goa-1*(*sa734*)::GOA-1::GFP (LX2071).

Table 2: Strains

Strains	Genotype	Available from
UN2301	*goa-1p*::GOA-1::TurboID	Cram lab

UN2306	*goa-1p*::TurboID	Cram lab
UN1108	*fln-1p*::GCaMP	Cram lab
LX2071	vsSi32 [goa-1::GFP + unc-119(+)] III	CGC

RNA interference

The RNAi protocol was performed as described previously (Kelley et al., 2020). *HT115(DE3)* bacteria (RNAi bacteria) transformed with a dsRNA construct of interest was grown overnight in Luria Broth (LB) supplemented with 40 µg/ml ampicillin and seeded (150 µl) on NGM plates supplemented with 25 µg/ml carbenicillin and disopropylthio-β-galactoside (IPTG). Seeded plates were left for 24–72 hours at room temperature (RT) to induce dsRNA expression. Empty pPD129.36 vector ("Control RNAi") was used as a negative control in all RNAi experiments.

Embryos from gravid adults were collected using an alkaline hypochlorite solution as described previously (Castaneda et al., 2020) and washed three times in M9 buffer (22 mM KH_2PO_4, 42 mM $NaHPO_4$, 86 mM NaCl, and 1 mM $MgSO_4$). Clean embryos were transferred to supplemented NGM plates seeded with HT115(DE3) bacteria expressing dsRNA of interest and left to incubate at 23°C for 50–56 hours depending on the experiment.

Spermathecal occupancy

To prepare age matched young adult animals for the spermathecal occupancy and transit assays, gravid hermaphrodites were lysed in an alkaline hypochlorite solution to release eggs, which were then placed onto seeded NGM plates and grown at 23°C for 52 hours. Animals were mounted on 5% agarose in 0.1 M sodium azide and observed immediately with DIC microscopy to score spermathecal occupancy rates. Imaging was performed on a Nikon Eclipse 80i microscope with a 60× oil-immersion lens using SPOT Advanced software (Version 5.3.5) and a charge-coupled device camera.

Biotinylation, western blotting, and mass spectrometry

Protein lysates were prepared from age-matched animals grown on *E. coli HT115(DE3)* carrying *goa-1p*::GOA-1::TurboID, *goa-1p*::TurboID and N2 as follows: Animals were washed from plates using M9 and allowed to settle and then frozen at -80°C. Animals were resuspended in RIPA lysis buffer containing protease inhibitors (Sanchez & Feldman, 2021). Protein extracts were obtained by sonication at 20% at 10 s intervals with 10 s breaks for 60 s total. The protein was quantified using the BCA Protein Assay Reagent. After adding the optimized volume of Pierce streptavidin-coated magnetic beads to 1 mg of protein for each sample, the lysate rotated gently on a slow spinning wheel at 4°C for 16 h. Then, the samples were washed multiple times with buffers (Sanchez & Feldman, 2021).

Samples were loaded onto Mini-PROTEAN TGX precast 10% polyacrylamide gels (Bio-Rad; Hercules, CA, USA) for SDS-PAGE. Antibodies used for Western blotting were Anti-Biotin Antibody at 1:1000 (SC-101339, Santa Cruz Biotechnology) for primary antibody, and donkey anti-mouse at 1:2000 (SA1100, Thermo Scientific Pierce) for secondary antibody.
The purified protein samples were analyzed using mass spectrometry to identify the proteins that were biotinylated. A list of proteins identified by mass spectrometry in three replicates is shown in Table 1.

Table 3: Antibodies

Antibody	Animal and clonality	Description
Anti-Biotin	Mouse	SC-101339, Santa Cruz Biotechnology

Donkey anti-mouse	Donkey	SA1100, Thermo Scientific Pierce

Image analysis and Statistics

ImageJ (FIJI) (version 2.16.0) was used for image analysis. GraphPad Prism (version 10.5.0) using Fishers exact t-test was employed for the statistical analysis.

Reference:

Bai, X., Bouffard, J., Lord, A., Brugman, K., Sternberg, P. W., Cram, E. J., & Golden, A. (2020). Caenorhabditis elegans PIEZO channel coordinates multiple reproductive tissues to govern ovulation. *eLife*, *9*, e53603. https://doi.org/10.7554/eLife.53603

Beg, A. A., Ernstrom, G. G., Nix, P., Davis, M. W., & Jorgensen, E. M. (2008). Protons act as a transmitter for muscle contraction in C. elegans. *Cell*, *132*(1), 149–160. https://doi.org/10.1016/j.cell.2007.10.058

Billington, C. K., Ojo, O. O., Penn, R. B., & Ito, S. (2013). cAMP regulation of airway smooth muscle function. *Pulmonary Pharmacology & Therapeutics*, *26*(1), 112–120. https://doi.org/10.1016/j.pupt.2012.05.007

Castaneda, P. G., Cecchetelli, A. D., Pettit, H. N., & Cram, E. J. (2020). Gα/GSA-1 works upstream of PKA/KIN-1 to regulate calcium signaling and contractility in the Caenorhabditis elegans spermatheca. *PLOS Genetics*, *16*(8), e1008644. https://doi.org/10.1371/journal.pgen.1008644

Howe, A. K. (2004). Regulation of actin-based cell migration by cAMP/PKA. *Biochimica et Biophysica Acta (BBA) - Molecular Cell Research*, *1692*(2–3), 159–174. https://doi.org/10.1016/j.bbamcr.2004.03.005

Huang, C. G., Lamitina, T., Agre, P., & Strange, K. (2007). Functional analysis of the aquaporin gene family in Caenorhabditis elegans. *American Journal of Physiology-Cell Physiology*, *292*(5), C1867–C1873. https://doi.org/10.1152/ajpcell.00514.2006

Jastrzebska, B. (2013). GPCR: G protein complexes—the fundamental signaling assembly. *Amino Acids*, *45*(6), 1303–1314. https://doi.org/10.1007/s00726-013-1593-y

Kelley, C. A., Triplett, O., Mallick, S., Burkewitz, K., Mair, W. B., & Cram, E. J. (2020). FLN-1/filamin is required to anchor the actomyosin cytoskeleton and for global organization of sub-cellular organelles in a contractile tissue. *Cytoskeleton*, *77*(10), 379–398. https://doi.org/10.1002/cm.21633

Kunkel, M. T., Johnstone, D. B., Thomas, J. H., & Salkoff, L. (2000). Mutants of a Temperature-Sensitive Two-P Domain Potassium Channel. *The Journal of Neuroscience*, *20*(20), 7517–7524. https://doi.org/10.1523/JNEUROSCI.20-20-07517.2000

Lee, J. H., Han, J. S., Kong, J., Ji, Y., Lv, X., Lee, J., Li, P., & Kim, J. B. (2016). Protein Kinase A Subunit Balance Regulates Lipid Metabolism in Caenorhabditis elegans and Mammalian Adipocytes. *Journal of Biological Chemistry*, *291*(39), 20315–20328. https://doi.org/10.1074/jbc.M116.740464

Sadeghian, F., Castaneda, P. G., Amin, M. R., & Cram, E. J. (2022). Functional Insights into Protein Kinase A (PKA) Signaling from C. elegans. *Life*, *12*(11), Article 11. https://doi.org/10.3390/life12111878

Sanchez, A. D., & Feldman, J. L. (2021). A proximity labeling protocol to probe proximity interactions in C. elegans. *STAR Protocols*, *2*(4), 100986. https://doi.org/10.1016/j.xpro.2021.100986

Torres-Quesada, O., Mayrhofer, J. E., & Stefan, E. (2017). The many faces of compartmentalized PKA signalosomes. *Cellular Signalling*, *37*, 1–11. https://doi.org/10.1016/j.cellsig.2017.05.012

Warnhoff, K., Murphy, J. T., Kumar, S., Schneider, D. L., Peterson, M., Hsu, S., Guthrie, J., Robertson, J. D., & Kornfeld, K. (2014). The DAF-16 FOXO Transcription Factor Regulates natc-1 to Modulate Stress Resistance in Caenorhabditis elegans, Linking Insulin/IGF-1 Signaling to Protein N-Terminal Acetylation. *PLOS Genetics*, *10*(10), e1004703. https://doi.org/10.1371/journal.pgen.1004703

A

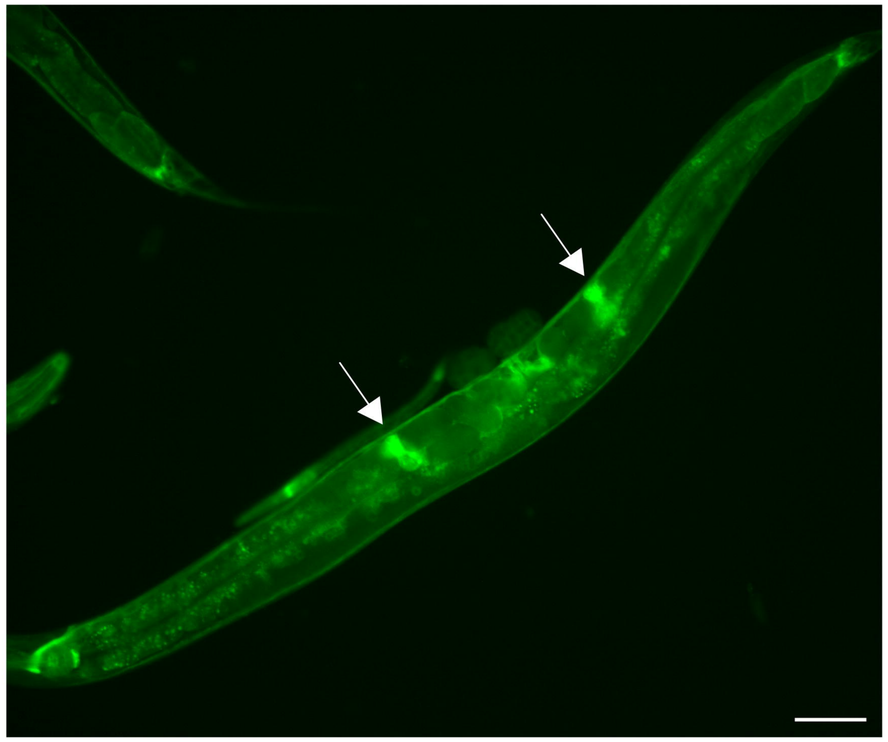

B

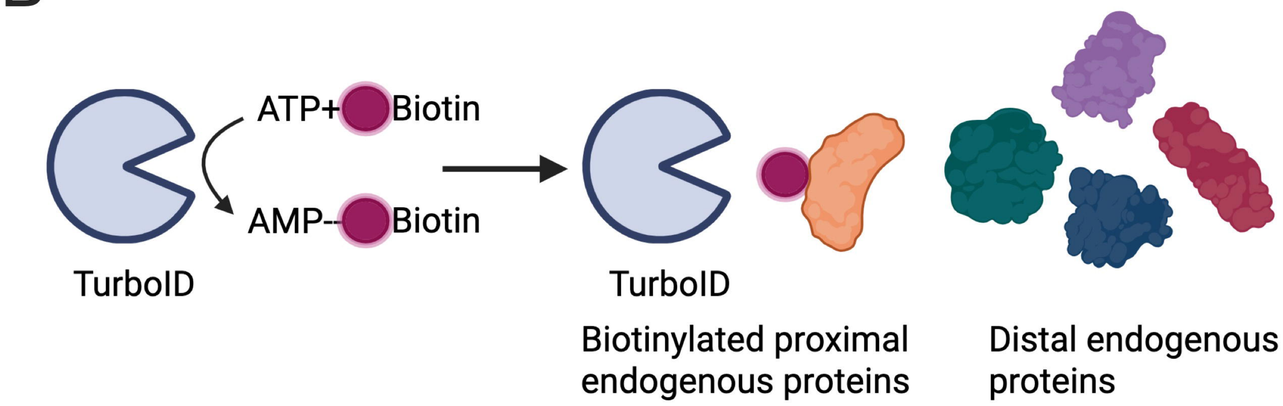
ATP+
Biotin
AMP--
Biotin
TurboID
TurboID
Biotinylated proximal endogenous proteins
Distal endogenous proteins

C

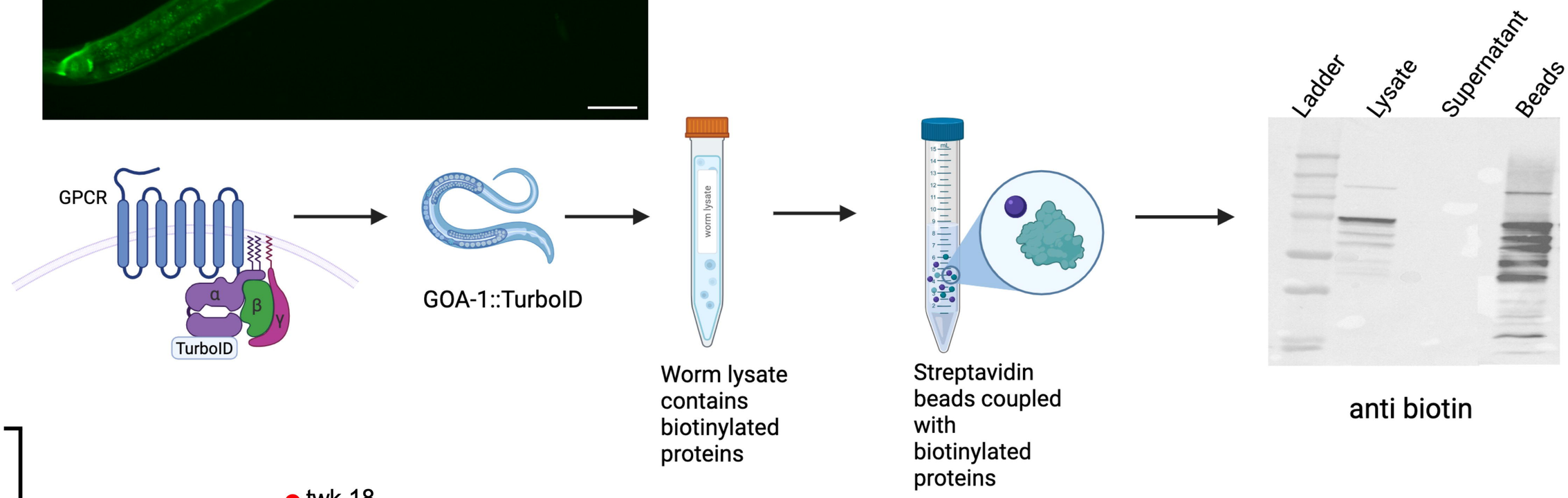
GPCR
α
β
γ
TurboID
GOA-1::TurboID
worm lysate
Worm lysate contains biotinylated proteins
Streptavidin beads coupled with biotinylated proteins
Ladder
Lysate
Supernatant
Beads
anti biotin

D

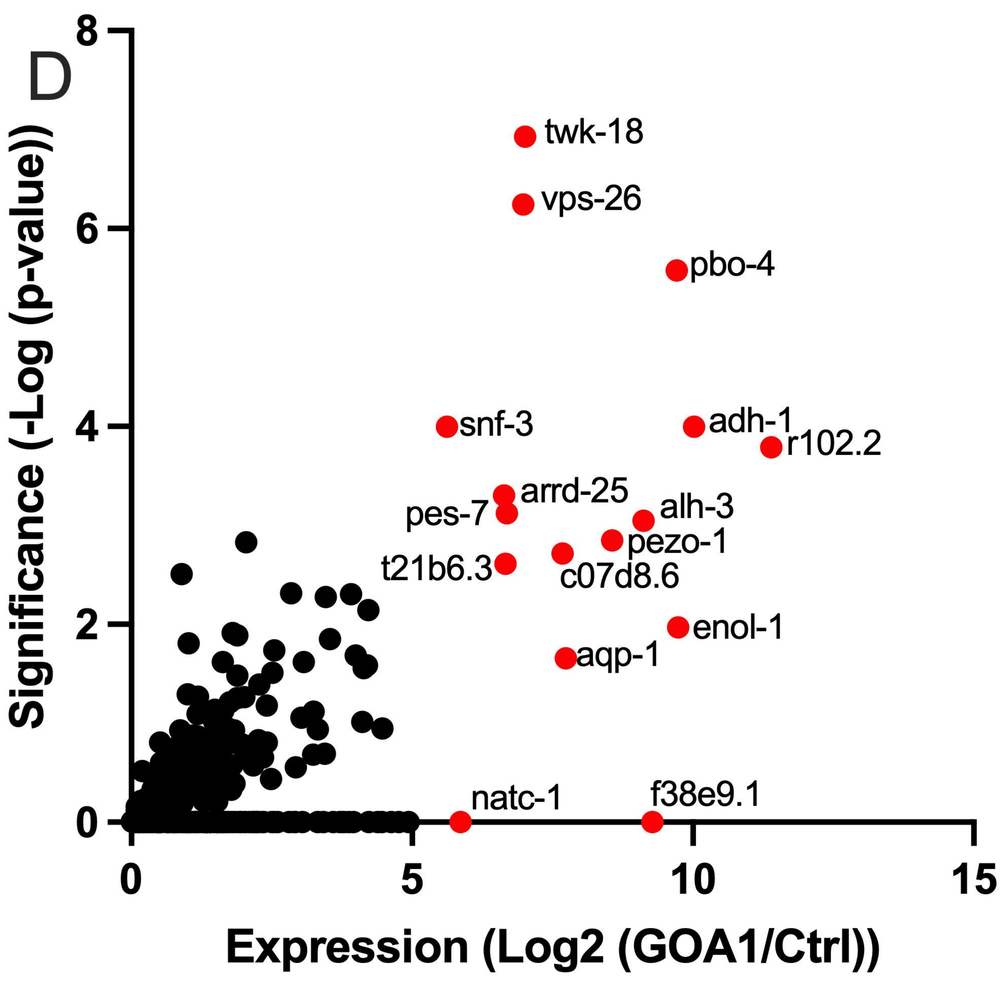
Significance (-Log (p-value))
Expression (Log2 (GOA1/Ctrl))
0
2
4
6
8
0
5
10
15
twk-18
vps-26
pbo-4
snf-3
adh-1
r102.2
arrd-25
pes-7
alh-3
pezo-1
t21b6.3
c07d8.6
enol-1
aqp-1
natc-1
f38e9.1

E

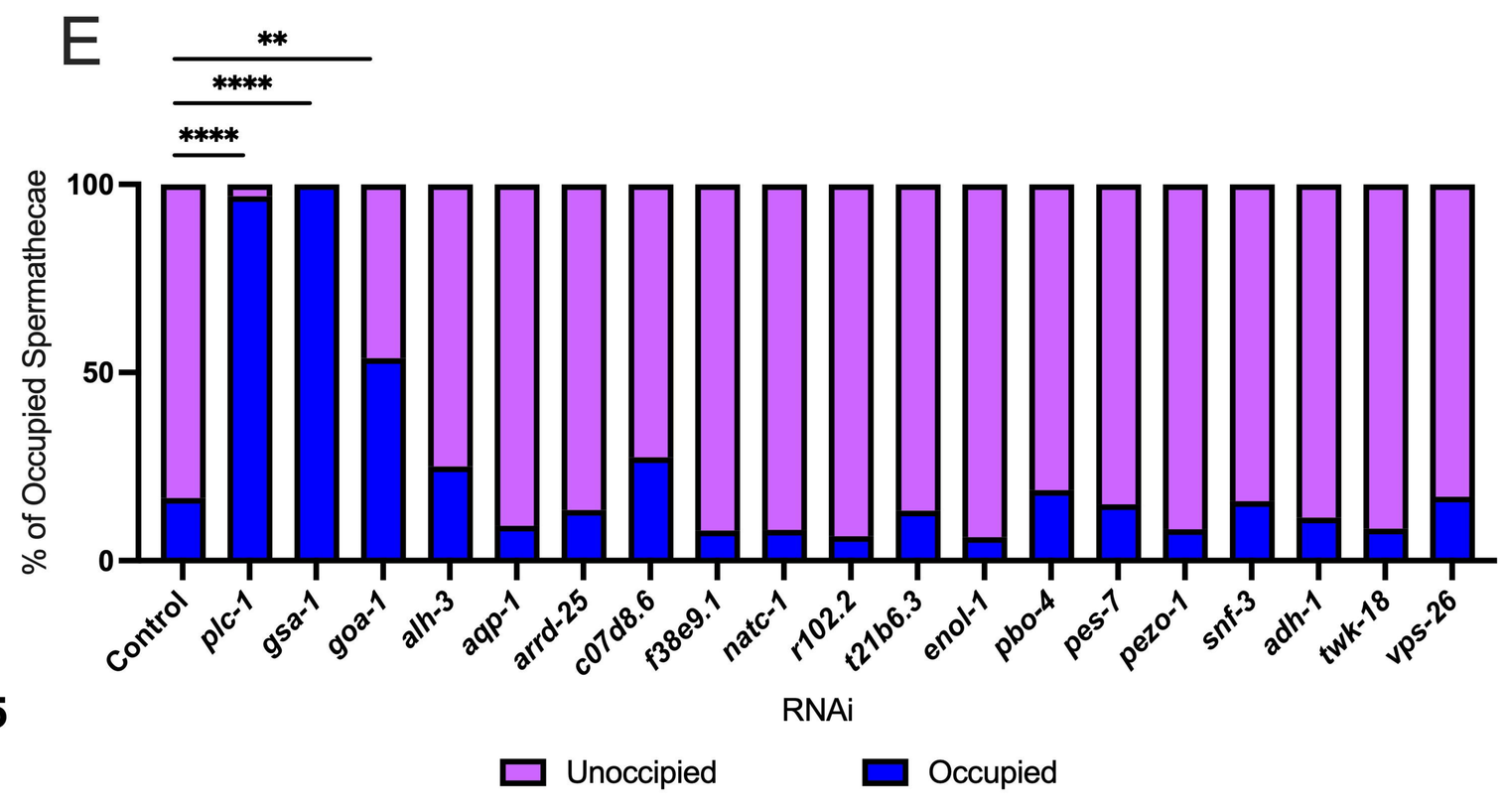
**
****
****
% of Occupied Spermathecae
100
50
0
Control
plc-1
gsa-1
goa-1
alh-3
aqp-1
arrd-25
c07d8.6
f38e9.1
natc-1
r102.2
t21b6.3
enol-1
pbo-4
pes-7
pezo-1
snf-3
adh-1
twk-18
vps-26
RNAi
Unoccipied
Occupied